



Purification-independent immunoreagents obtained by displaying nanobodies on bacteria surface

Sandra Oloketuyi¹ · Carina Dilkaute² · Elisa Mazzega¹ · Joachim Jose² · Ario de Marco¹

Received: 14 December 2018 / Revised: 29 March 2019 / Accepted: 1 April 2019 / Published online: 15 April 2019
© Springer-Verlag GmbH Germany, part of Springer Nature 2019

Abstract

The availability of preimmune libraries of antibody fragments allows for the fast generation of binders which can be expressed in both eukaryotic and prokaryotic systems. We exploited the recombinant nature of antibody fragments to demonstrate the possibility of expressing them as functional proteins displayed on the surface of *Escherichia coli* and by such a way to generate living reagents ready-to-use for diagnostics. Such immunoreagents were effectively exploited without the necessity of any purification step to prepare immunocapture surfaces suitable for the diagnostic of both cancer cells and toxic microalgae. The same nanobody-displaying bacteria were also engineered to coexpress GFP in their cytoplasm. Suspensions of such living fluorescent immunoreagents effectively bound to eukaryotic cells making them visible and quantifiable by flow cytometry analysis and using 96-well plate readers. The collected data showed the suitability of such living immunoreagents for reproducible and inexpensive diagnostic applications.

Keywords Antibody functionalization · Bacterial display · Nanobodies · Diagnostics · Toxic microalgae

Introduction

Recombinant antibody fragments are a convenient alternative to conventional IgG molecules because they are easy to engineer and can be produced inexpensively in prokaryotic systems. Preimmune libraries of nanobodies provided binders against tens of different antigens (Monegal et al. 2009; Moutel et al. 2016; Crepin et al. 2017a; Crepin et al. 2017b) and the nanobody sequences recovered by panning can be fused to tags such as 6xHis, GFP, Fc, or free cysteine which simplify their purification, derivatization, and application in flow cytometry, in vitro and in vivo imaging, as well as in the

preparation of biosensors and nanoparticles (Veggiani et al. 2011; Djender et al. 2014; Zou et al. 2015; Ambrosetti et al. 2017). Nevertheless, such immunoreagents have highly variable stability and degradation problems. Their functional yields can be sometimes insufficient for downstream applications (Veggiani and de Marco 2011; Djender et al. 2014). It would be therefore meaningful to develop production protocols able to maximize antibody yields and stability and at the same time could shorten the purification procedure. Display of different recombinant proteins on various bacteria represents a convenient and highly validated means for creating functional reagents and biocatalysts without the necessity to isolate active proteins (Shao et al. 2009; Wiczorek and Martin 2010; Nhan et al. 2011; Gustavson et al. 2011; Jong et al. 2012; Schürmann et al. 2014; Sührer et al. 2015; Tozakidis et al. 2015) as well as for sorting specific binders during panning (Fleetwood et al. 2013; Salema et al. 2016). Also, functionally active binders were successfully displayed on lactobacilli and *E. coli* (Krüger et al. 2002; Marcotte et al. 2006; Fleetwood et al. 2014) and therapeutic *Salmonella* cells displaying nanobodies were used for targeted delivery in vivo (Massa et al. 2013), but the potential of antibody-displaying bacteria as diagnostic reagents was rarely exploited (De Marni et al. 2012; Bong et al. 2018). In this work, we describe the applications of *E. coli* designed to display nanobodies on their

Electronic supplementary material The online version of this article (<https://doi.org/10.1007/s00253-019-09823-x>) contains supplementary material, which is available to authorized users.

✉ Ario de Marco
ario.demarco@ung.si

¹ Laboratory of Environmental and Life Sciences, University of Nova Gorica, Vipavska cesta 13, SI-5000, Rožna Dolina, Nova Gorica, Slovenia

² Institut für Pharmazeutische und Medizinische Chemie, PharmaCampus, Westfälische Wilhelms-Universität Münster, Corrensstr. 48, 48149 Münster, Germany

surface to create “diagnostic living bacteria.” These were exploited for building both immune-capturing surfaces and soluble detection fluorescent reagents. Diagnostic bacteria can be prepared straightforward by inducing the nanobody display at the cell surface—and eventually the expression of a fluorescent protein in the cytoplasm—followed by bacteria recovery by centrifugation. This solution significantly reduces time and costs for the production of recombinant antibodies for immune affinity assays and, interestingly, also optimizes their outwards orientation and accessibility at the bacterial surface (Michon et al. 2016).

Material and methods

Plasmid construction

Three different plasmids were constructed for the expression of fusion proteins comprising the nanobody and the autotransporter elements using the restriction-free In-Fusion strategy (Berrow et al. 2007). The nucleotide sequences of the three nanobodies A10 (Djender et al. 2014), C1 (Mazzega et al. 2018), and H6 (Popovic et al. 2018) were amplified via PCR. These sequences were then used to replace the passenger DNA sequence in the autotransporter fusion gene MATE (Sichwart et al. 2015). The resulting clone encoded an N-terminal CtxB signal peptide, the nanobody, and a C-terminal autotransporter domain which derives from the EhaA autotransporter from *E. coli* strain O157:H7 [GenBank Accession No. Q8X6C1]. Such DNA sequences were cloned in the pBAD/gIII vector (Thermo Scientific, Braunschweig, Germany), the expression of which is under the control of the arabinose-inducible araBAD promoter. The three plasmids were termed pBAD-MATE A10, pBAD-MATE C1, and pBAD-MATE H6 (Supplementary Material, Table S1).

The plasmid pJS009 consisted of the same autotransporter vector but in combination with the DNA sequence of formate dehydrogenase (FDH), a codon-optimized variant based on the FDH from *Mycobacterium vaccae* N10 (Hoelsch et al. 2013) and obtained by artificial gene synthesis (GeneArt, Regensburg, Germany). The plasmid pKE19 encoding GFP has already been described before (Yoo et al. 2011; Quehl et al. 2017) (Supplementary Material, Table S1).

Proof of VHH bacterial display and GFP expression

The *E. coli* strain UT5600(DE3) (Jose and Handel 2003) was transformed with the plasmid pBAD-MATE containing the sequence encoding the autotransporter domain of EhaA fused either to the sequence corresponding to a VHH or to the sequence of formiat dehydrogenase (FDH) as a passenger. The resulting strains were transformed with a second plasmid

encoding GFP (pKE19). Whereas the expression of the autotransporter fusion proteins was controlled by an arabinose-inducible promoter, expression of GFP was constitutive. All strains were grown in LB medium supplemented with 10 μ M EDTA, 15 mM 2-mercaptoethanol and the required antibiotics (50 μ g/mL carbenicillin, 30 μ g/mL chloramphenicol) at 37 °C and 200 rpm. At an optical density (OD_{578}) of 0.5, protein expression was induced by addition of arabinose to a final concentration of 0.2%. Induction was carried out at 23 °C and 200 rpm for 16 h. Surface display was verified by the fusion protein accessibility to proteinase K. An aliquot of intact cells was treated with proteinase K at 37 °C for 1 h, and afterwards, outer membrane protein fractions were prepared according to the protocol of Park et al. (2015). The outer membrane proteins of treated and intact cells were separated by SDS-PAGE and stained with Coomassie Brilliant Blue. For flow cytometric analysis, an aliquot of 500 μ L cell suspension was harvested (1 min, 14,000 \times g) and washed three times with filtered PBS. Finally, 50,000 cells per sample were analyzed.

Evaluation of bacterial adhesion and diagnostics based on nanobody-displaying bacteria

Titanium dioxide (TiO_2) powder with diameter of 25, 50, and 100 nm (Aeroxide) was suspended in absolute ethanol to the final concentrations of 0.25, 0.5, and 1 mg/mL for each of the three compounds. To avoid possible aggregation and maximize size uniformity, the suspensions were sonicated 20 min in a water bath (Elmasonic). Polystyrene plastic microplate wells (Greiner 96 Flat Bottom Black Chimney Well High Binding - 655077; Greiner 96 Flat Bottom Clear Microlon High Binding - 655081; Sarstedt Standard 96 Flat Bottom Standard - 83.3924) were coated with 200 μ L of the TiO_2 suspensions and oven-dried at 60 °C overnight.

E. coli bacteria BL21(DE3) SOX (Djender et al. 2014) transformed with the vector pETM14 for GFP expression were inoculated into 25 mL of LB medium plus 100 μ g/mL ampicillin, cultured at 37 °C and 220 rpm and induced at OD_{600} of 0.4 with 0.2 mM IPTG. Then, the temperature was decreased to 20 °C and bacteria were incubated overnight. For preliminary assessment of bacterial adhesion to TiO_2 -coated microplates, cells were resuspended in PBS to reach an OD_{600} of 0.3 and 100 μ L of the cell suspension were directly spotted into microplate wells previously coated with TiO_2 . The microplates were incubated for 48 h at 37 °C and 220 rpm. After incubation, wells were washed three times with 1 \times PBS and fluorescence intensity was measured at 488 nm using a microplate reader (Tecan Infinite F200). The effect of centrifugation on adhesion efficiency was evaluated by comparing the data from two sets of microplates used in parallel: (a) the microplates were incubated 24 h at 37 °C and 220 rpm; (b) the microplates were immediately centrifuged at 1109 \times g for

10 min (Beckman Coulter Allegra), the supernatant was removed and the bacterial pellet resuspended in 100 μL of LB supplemented with suitable antibiotics before being cultured as in (a). After incubation, wells were washed 15 times with $1\times$ PBS. Fluorescence intensity was measured at 488 nm using a microplate reader (Tecan Infinite F200) after each washing step. Given the extremely high number of generated combinations, each one was tested only twice to confirm the value trends and then a representative dataset was reported without statistical analysis.

The assessment of the adherence characteristics of displaying bacteria was performed by analyzing different expression combinations. The plasmids pKE19 (constitutive cytoplasmic GFP expression), pJS009 pKE19 (expression of cytoplasmic GFP plus surface display of the control protein FDH), pBAD-MATE A10 pKE19, pBAD-MATE C1 pKE19, and pBAD-MATE H6 pKE19 (expression of cytoplasmic GFP plus surface display of VHH A10, C1, and H6, respectively) were used to transform individually or in combination the *E. coli* strain UT5600(DE3) (S1). The resulting strains were used to inoculate 5 mL of LB medium supplemented with appropriate antibiotics (100 $\mu\text{g}/\text{mL}$ ampicillin with or without 25 $\mu\text{g}/\text{mL}$ chloramphenicol). Aliquots of 0.5 mL of bacteria cultured overnight at 37 °C and 200 rpm were used to inoculate 50 mL of LB medium supplemented with required antibiotic(s) and 10 μM EDTA. Bacteria were initially grown at 37 °C, 200 rpm, and recombinant expression was induced at an OD_{600} of 0.6 by the addition of L-arabinose (0.2% w/v). The temperature was decreased to 23 °C. Bacteria were incubated overnight before being harvested (3.214 \times g for 10 min using an Eppendorf 5804 centrifuge) and washed twice with $1\times$ PBS at same centrifugation speed and time. Cells were further resuspended in PBS at OD_{600} of 0.3 and 0.5 before being spotted (100 μL) on plastic microplates with or without TiO_2 coating, as described above.

The bacteria displaying the same proteins were used for assessing their immunocapture efficiency. Bacteria were first incubated in the microplate (100 $\mu\text{L}/\text{well}$, OD_{600} of 0.3) overnight at 23 °C and 150 rpm, then blocked 3 h at 4 °C with 100 $\mu\text{L}/\text{well}$ of 1% (w/v) BSA in PBS and finally washed twice with $1\times$ PBS. Mammalian cells (SKBR3, MDA-MB231, and HEK293) were blocked with PBS plus 1% BSA for 1 h at 4 °C. One hundred microliters of blocked mammalian cell suspension (5×10^4 cells/well) were added to the blocked bacterial cells, incubated for 1 h at 4 °C and washed thrice with $1\times$ PBS. One hundred microliters of bacteria expressing cytoplasmic GFP and displaying the anti-HER2 nanobody A10 ($\text{OD}_{600\text{nm}}$ of 0.3) were added to each well and incubated for 1 h at 4 °C. After GFP bacteria removal, wells were washed twice with $1\times$ PBS and once with PBS plus 0.1% Triton X-100. The immunoreaction was quantified measuring the fluorescence intensity as above. The same protocol was applied to fixed algal cells (*Alexandrium minutum*

and *Scipisiella* spp.: COsMi strains 1005 and 1049, respectively, at <http://cosmi.inogs.it/>) with the only difference that bacteria used for capture and detection displayed the anti-A. *minutum* C1 nanobody. When fluobodies were used for staining the captured cells, 100 μL of a 5 $\mu\text{g}/\text{mL}$ stock solution were exploited.

Fluorescence microscopy

E. coli cells cotransformed for expressing cytoplasmic GFP and surface displayed nanobodies were grown in LB medium supplemented with 10 μM EDTA, 15 mM 2-mercaptoethanol, 50 $\mu\text{g}/\text{mL}$ carbenicillin, and 30 $\mu\text{g}/\text{mL}$ chloramphenicol at 37 °C and 200 rpm. At an OD_{600} of 0.5, gene expression was induced by addition of arabinose to a final concentration of 0.2%. Induction was carried out for 1 h at 30 °C and 200 rpm. Cells were harvested (4470 \times g, 3 min) and washed with PBS twice. The OD_{578} was adjusted to 5.

The BT-474 cells were grown on sterile coverslips placed at the bottom of a 6-well plate using 200,000 cells per well seeded in 2 mL of medium [80% (v/v) RPMI 1640-Medium, 20% (v/v) FCS and 10 $\mu\text{g}/\text{mL}$ human insulin]. Cells were incubated for 48 h at 37 °C and 5% CO_2 before being washed with 1 mL PBS per well and fixed with 1 mL paraformaldehyde 3% (v/v) solution in PBS for 15 min. The coverslips were washed twice with PBS and permeabilized with Triton X-100 [0.3% (w/v) in PBS] for 20 min. After two further PBS washing steps, cells were stained with Hoechst 33342 for 30 min. The coverslips were washed two more times, and 1 mL of PBS was added to each well, as well as 200 μL of the bacterial cell suspension. The fixed and stained BT-474 cells were incubated with the nanobody-presenting bacteria for 1 h at 37 °C and 200 rpm. Afterwards, the coverslips were washed with PBS and water before being mounted with DABCO/Mowiol on glass slides. The samples were examined by fluorescence microscopy (Keyence BZ-9000).

Fluobody preparation

Fluobodies formed by the fusion of VHH and GFP were expressed and purified as previously described (Mazzega et al. 2018). Specifically, the sequences corresponding to the nanobodies A10 and C1 were inserted into a modified pET14b vector to generate eGFP-nanobody fusion constructs with a C-term 6xHis tag suitable for affinity purification. The construct expression was performed in the cytoplasm of *E. coli* BL21 (DE3) SOX strain (Veggiani and de Marco 2011) growing the bacteria in LB medium at 250 rpm and 37 °C until $\text{OD}_{600\text{nm}}$ reached the value of 0.4. Then, temperature was lowered to 20 °C and L-arabinose was added to the final concentration of 0.5% (w/v) to induce sulfhydryl oxidase and DsbC expression. After 30 min, IPTG (0.5 mM) was added to induce the antibody construct expression and the

bacteria were grown overnight. Cells were pelleted by centrifugation, resuspended in lysis buffer (50 mM TrisHCl pH 8, 500 mM NaCl, 2.5 mM MgCl₂, 0.5 mg/mL lysozyme and 3 U DNase I) sonicated on ice (3 times × 30 s), and after 30 min of incubation, the supernatant was collected after lysate centrifugation. Affinity purification was performed by means of a 5 mL HiTrap TALON® column in combination with a chromatographic AKTA pure system (GE Healthcare). Purified fluobodies were separated by denaturing SDS-PAGE and stained with colloidal blue. Protein concentration was determined by Bradford assay.

Flow cytometry experiments

Exponentially growing cells of *Alexandrium minutum* were washed twice with PBS and blocked with 5% BSA for 40 min before being resuspended in PBS at a concentration of 1 million/mL. Aliquots of 100 µL, corresponding to 10⁵ live cells, were used for each experiment in combination with 100 µL of bacteria (OD_{600nm} of 0.3) expressing cytoplasmic GFP and displaying the C1 nanobody. As a positive control, the same amount of *A. minutum* cells was stained with 1 µg of purified C1-GFP fluobody (Mazzega et al. 2018). As a negative control, cells were incubated with either 100 µL of PBS or 100 µL of bacteria expressing cytoplasmic GFP and displaying an irrelevant protein. Samples were incubated in the darkness for 2 h at 4 °C, washed twice with PBS, resuspended in 300 µL of PBS and finally processed for flow cytometry analysis by using a FACSCanto II instrument (BD Biosciences) equipped with a blue solid-state 20-mW laser (excitation at 488 nm) and a 17 mW red laser (excitation at 640 nm). GFP was monitored using the FITC filter (530 nm), whereas pigment autofluorescence was monitored with the PerCP-Cy5 filter (670 nm). The *A. minutum* population was gated on the PerCP-Cy5/SSC plot and specific bacterial binding to *A. minutum* cells was monitored by means of the GFP signal. For each sample, at least 10,000 events were recorded in the target cell gate. Data files were acquired and analyzed by using FACSDiva (BD Biosciences) and Flowing Software 2.5.1 (CyFlo Ltd., Finland). References for fluorescence intensities of the controls and gating conditions are reported in Fig. S5.

Results

Recombinant monoclonal antibodies can be easily engineered into reagents provided with tags designed for simplifying the downstream applications (Aliprandi et al. 2010; Djender et al. 2014). The option of displaying recombinant nanobodies on (fluorescent) bacteria was evaluated as a further engineering opportunity and a means to produce “living immunoreagents” designed for the capture and detection of relevant biological targets

without requiring purification prior to their employment. The approach was evaluated with nanobodies fused to the autotransporter EhaA and which recognize membrane antigens exposed on human tumor cells, toxic microalgae, and extracellular vesicles (Djender et al. 2014; Mazzega et al. 2018; Popovic et al. 2018). These binders were expressed under the control of an arabinose-inducible promoter in both wt UT5600(DE3) bacteria and in the same bacteria cotransformed with the plasmid pKE19 for constitutive GFP expression (Table S1) (Yoo et al. 2011; Quehl et al. 2017). Consequently, for each nanobody, we obtained couples of displaying bacteria, a non-colored version designed for immune-capture and a second one that was fluorescent and suitable for being used as a reporter.

The efficiency of nanobody display was assessed by exploiting the capacity of proteinase K to cleave accessible substrates exposed on the external bacterial surface. Nanobody removal was compared with that of the enzyme formiat dehydrogenase (FDH) used as a control. Outer membrane proteins from treated and untreated cells were isolated and separated by SDS-PAGE (Fig. 1a). Data clearly showed that all the recombinantly displayed proteins were digested by the proteinase, which is a strong hint for a surface exposure of the passenger. To exclude that proteinase K had entered the periplasm, the native outer membrane protein OmpA (35 kDa) was considered. If proteinase K enters the cell, the periplasmic domain of OmpA will be digested leading to the disappearance of the OmpA band. As the OmpA band was not vanishing in the corresponding experiment, the surface exposure of the nanobodies is confirmed. They were correctly secreted and anchored at the external side of the bacterial membrane (Park et al. 2015). The functionality of the displayed nanobodies was assessed by incubating *E. coli* cells made fluorescent by cytoplasmic GFP expression and displaying either the anti-HER2 nanobody A10 (positive control) or the H6 irrelevant nanobody (negative control) at their surface in combination with HER2-expressing BT-474 cells. The sample examination at the fluorescence microscope showed that only the *E. coli* cells displaying the anti-HER2 nanobody at their surface were able to bind to BT-474 cells whereas the bacteria displaying the control nanobody showed no unspecific binding (Fig. 1b).

The yields of autotransporter fusion proteins clearly differed and, at least in two cases, were negatively influenced by the concomitant coexpression of GFP (Fig. 1a). Flow cytometry analysis of the GFP expressing bacteria indicated that cells were significantly brighter with respect to controls, whereas inside each single bacterial population, the fluorescence intensity had a relatively wide distribution (Fig. 1c). Effects of competition among coexpressed recombinant proteins, expressed both intracellularly and as surface displayed constructs, have been reported before (de Marco et al. 2007; Kranen et al. 2014; Gratz et al. 2015; Quehl et al. 2016) and are reproducible.

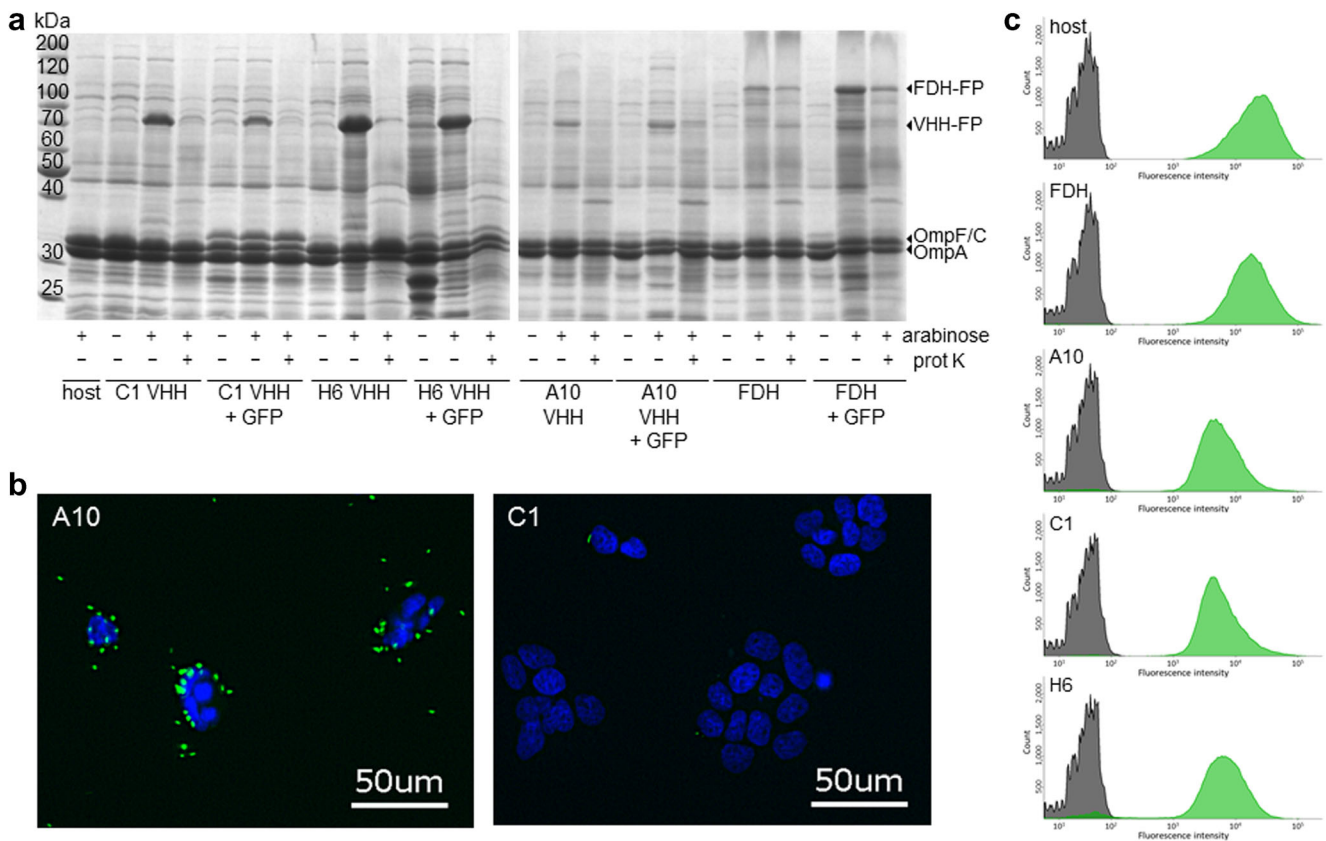


Fig. 1 Characterization of nanobodies displayed on bacterial surface. **a** Analysis of the expression and protease accessibility of the displayed fusion proteins by SDS-PAGE. The position of the VHH and FDH fusion proteins (VHH-FP, FDH-FP) is marked with an arrow. **b** Binding of nanobody-displaying *E. coli* cells to BT-474 tumor cells. HER2-

positive BT-474 cells grown on coverslips were stained with Hoechst 33342 and incubated with *E. coli* cells displaying either the anti-HER2 nanobody A10 (left) or the negative control nanobody C1 (right). **c** Analysis of GFP accumulation by flow cytometry. The data show the actual GFP content in the cell populations transformed for protein display

Once demonstrated the feasibility to display the nanobodies on the bacteria, we tried to optimize the bacteria adhesion on solid surfaces and to evaluate whether protein display could affect this process. We systematically evaluated the factors affecting the bacterial adhesion on both, commercial plastic plates and surfaces treated with TiO₂ (Fig. 2 and Figs. S1 and S2) (Lorenzetti et al. 2015; Chauhan et al. 2016), by using bacteria made fluorescent by cytoplasmic GFP expression. Bacterial adhesion efficiency/stability was inferred by measuring the fluorescence signal of the treated microplate wells at each processing step. Three microtiter plates with different surface characteristics, treated with TiO₂ powders of different diameters and used at three different concentrations (see “Material and methods” for details) were compared. The results relative to the adhesion of bacteria on Greiner 96 Flat Bottom Black Chimney Well High Binding – 655077 have been reported as an example in Fig. 2. This first set of data (absolute fluorescence intensities normalized by subtracting the blank values) confirmed that some combinations could substantially increase bacterial resistance to repeated washing steps. First, the combined effect of TiO₂ powder diameter, concentrations, and washing was evaluated 24

and 48 h after bacterial addition, and the best results in terms of adhesion stability were obtained with the P50 and P100 powders (Fig. 2a). A preliminary bacteria pelleting followed by resuspension in fresh LB medium was performed to evaluate possible interference of medium by-products on the bacterial adherence capacity. The process required an extra centrifugation step and was avoided since resulted in lower adhesion capacity when evaluated by measuring the variation of fluorescence signal after each of 15 successive washing steps using 100 μL of GFP-fluorescent bacteria at an OD₆₀₀ of 0.3 (Fig. 2b). By comparing the data reported in Fig. 2a, b with those acquired using the same experimental conditions but in combinations with the other microplates (Figs. S1 and S2), it was possible to determine that Sarstedt Standard 96 Flat Bottom Standard – 83.3924 was the most suitable for the application. We finally evaluated the effects of protein display and bacterial density on the adhesion stability of the bacteria. Even though the nanobody display apparently contributed to decrease bacterial adhesion independently of the surfaces used (Fig. 2c and Fig. S3), it was possible to select coating conditions that enabled relatively high and stable binding to use in the successive experiments. The chosen combination foresaw

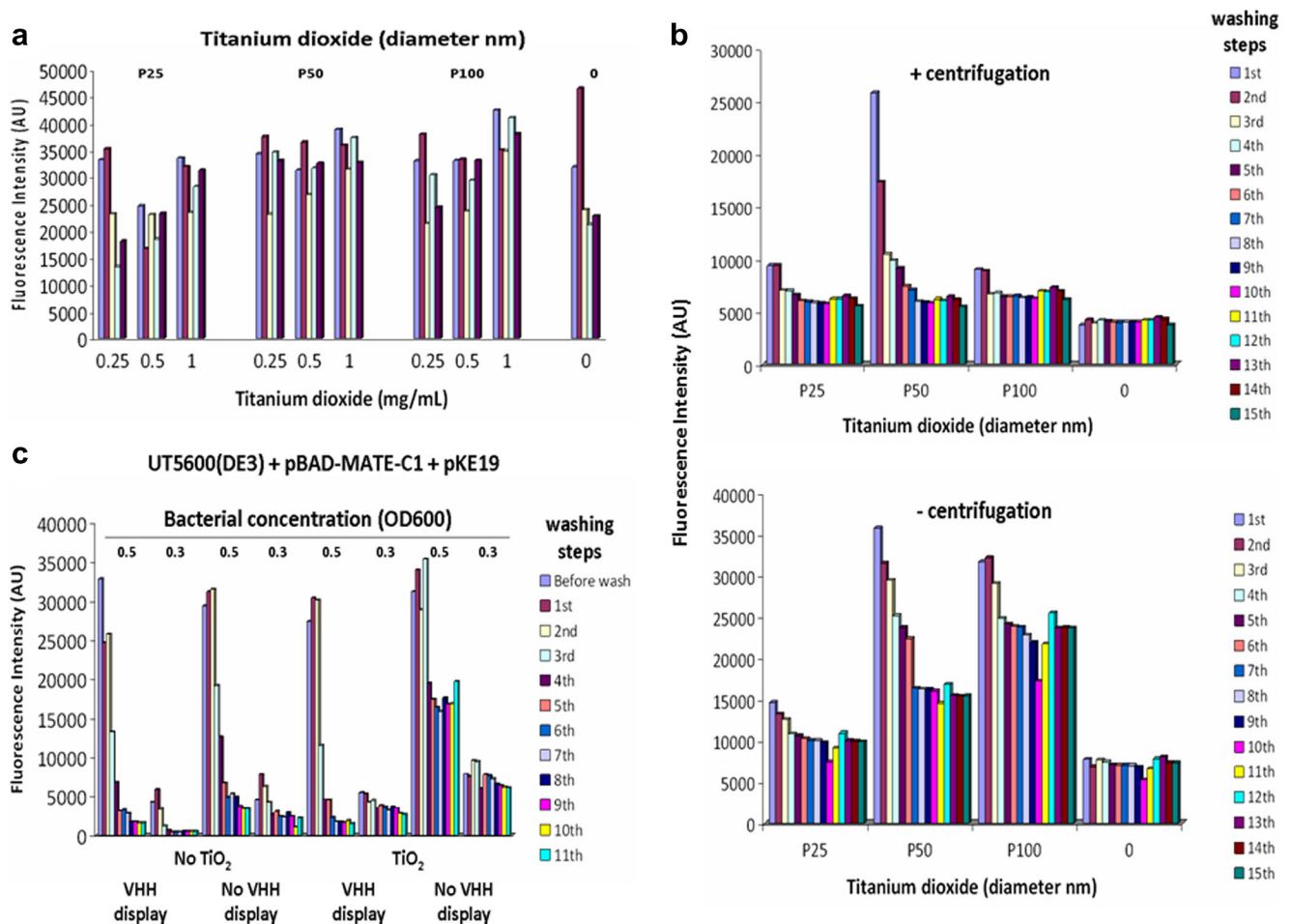


Fig. 2 Characterization of bacteria adhesion on plastic microplates. Data refer to the Greiner 96 microplate Flat Bottom Black Chimney Well High Binding. **a** Plates were treated with TiO₂ powders of different diameter (P25, P50, P100) at three concentrations (0.25, 0.5, 1 mg/mL). For each sample, the fluorescence of GFP-expressing bacteria was measured after 5 processing steps (time 0, after 24 h of incubation, 24 h plus washing, 48 h of incubation, 48 h plus washing). **b** The effect of initial bacterial centrifugation on fluorescence signal stability was assessed over 15

washing rounds using GFP-expressing bacteria at OD₆₀₀ = 0.3 plated on wells treated with 0.5 mg/mL of TiO₂ powder. **c** Evaluation of the bacteria concentration (OD₆₀₀ of 0.3 and 0.5) and nanobody display effects on bacterial adhesion on plastic and TiO₂-treated surfaces. The comparison was performed between green fluorescent (pKE19) bacteria UT5600(DE3) without and with display of the anti-microalgae C1 VHH (by means of pBAD-MATE)

the Sarstedt Standard 96 Flat Bottom Standard – 83.3924 plate treatment with 0.5 mg/mL of P50 TiO₂ and the employing of non-centrifuged bacteria at a concentration corresponding to the OD₆₀₀ of 0.3. We also noticed that in some experiments, the fluorescence intensity increased with the time despite the repeated washing steps (Fig. S2). In the past (De Marni et al. 2012), we noticed that spotted bacteria still grow on the surface on which they adhere and this resulted in stronger signals after 5 weeks of incubation. Therefore, the two opposite effects (bacterial removal by washing and bacterial growth) will determine a dynamic equilibrium according to the relative adhesion strength provided by the different surfaces.

Next, we assessed the possibility to exploit nanobody-displaying bacteria to selectively capture and detect mammalian cells. Non-fluorescent bacteria displaying anti-HER2 nanobodies were used to coat the wells of a TiO₂-treated

microtiter plate, incubated with HER2 pos and HER2 neg mammalian cells (SKBR3 and MDA-MB231, respectively) and finally with fluorescent bacteria displaying anti-HER2 nanobodies. Controls were performed to evaluate any kind of possible unspecific binding, and finally, the fluorescence was quantified by means of a spectrophotometer (Fig. 3a). The data show that only the specific combination (sandwich composed by anti-HER2 displaying bacteria for both capture and detection in the presence of HER2 pos SKBR3 cells, Fig. 3b) gave a strong signal (roughly 4.000 AU). This signal was significantly above the background (around 1.000 AU) that remained constant for all the controls. As expected, A10-captured SKBR3 cells were not visualized by GFP bacteria exposing irrelevant proteins such as the enzyme FDH and the anti-algal VHH C1, neither bacteria displaying irrelevant nanobodies (C1) succeeded in capturing SKBR3 cells (Fig.

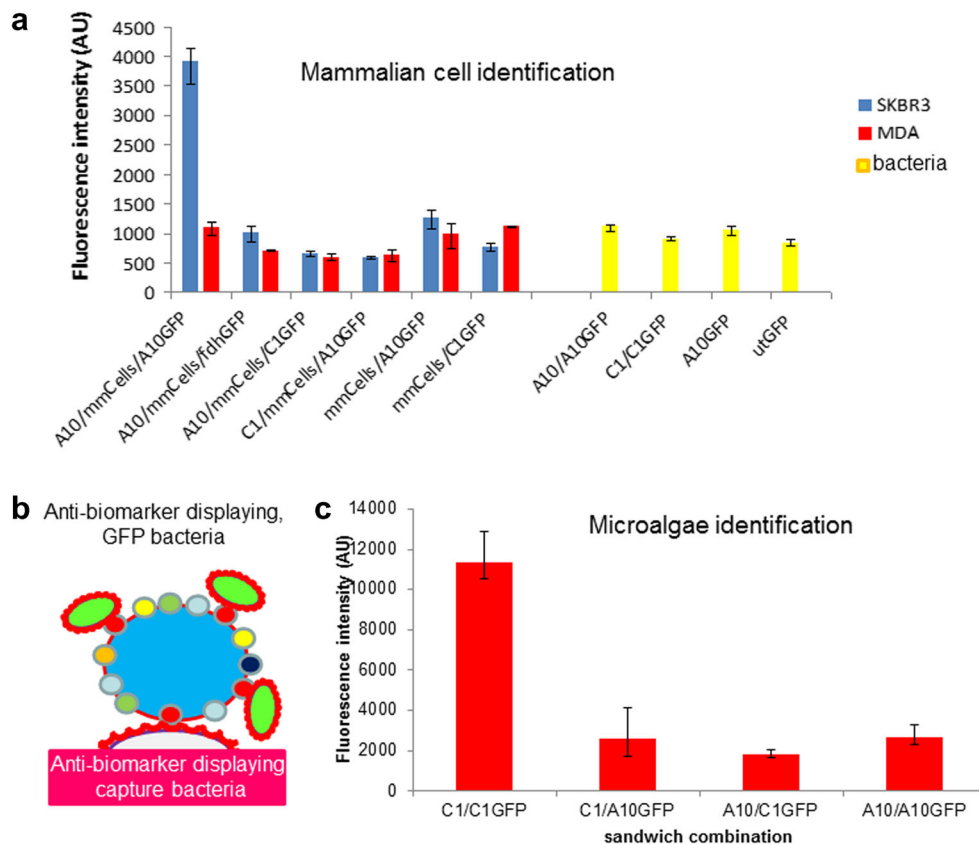


Fig. 3 Selective immunocapture and detection of target cells by bacteria displaying nanobodies. **a** Non-fluorescent bacteria displaying the anti-HER2 nanobody A10 (capturing bacteria) were incubated with HER2 pos (SKBR3) and HER2 neg (MDA-MB231) mammalian cells. As detection reagents, fluorescent bacteria displaying the same anti-HER2 nanobody (detection bacteria) were used. Controls were (i) detection bacteria displaying the irrelevant enzyme FDH; (ii) detection bacteria displaying the irrelevant nanobody C1 (anti-microalgae VHH); (iii) capturing bacteria displaying the irrelevant nanobody C1; (iv) absence of capture bacteria; (v) absence of capture bacteria and detection bacteria displaying the irrelevant nanobody C1; (vi–vii) absence of mammalian cells; (viii–ix) absence of both capture bacteria and mammalian cells, only GFP detection bacteria displaying either anti-HER2 nanobodies or

no protein, respectively. **b** Biological relevant cells (cancer cells, toxic microalgae) can be immune-captured for quantification using non-colored bacteria displaying nanobodies specific for antigens expressed at the surface of the target cells. Once immobilized, target cells are visualized by means of fluorescent bacteria displaying suitable nanobodies specific for cell surface antigens. **c** Non-fluorescent bacteria displaying the anti-*A. minutum* nanobody C1 (capturing bacteria) were incubated with *A. minutum* cells. As detection reagents, fluorescent bacteria displaying the same C1 nanobody (detection bacteria) were used. As controls, C1-captured cells were incubated with A10-displaying (anti-HER2) GFP detection bacteria and A10-displaying bacteria were used for capturing *A. minutum* cells in combination with GFP-bacteria displaying either A10 or C1 nanobodies

3a). Interestingly, the immune capture of mammalian cells by A10-displaying bacteria seemed to be crucial for stable binding of the HER2 pos cells at the used experimental conditions, probably because it prevented the loss of cells during repeated washes. According to the fluorescence values reported in Fig. 3a, it seems that cells which were pelleted by simple standard centrifugation (no immunocapture) were critically lost during washing. Displaying bacteria used in different combinations in the absence of mammalian cells gave only background fluorescence values below 1000, indicating that there was no unspecific binding of such reagents to the well surfaces. When Triton X-100 was added to PBS to increase the stringency of the washing steps (Fig. 4), fluorescence values decreased proportionally in all the samples but the signal-to-noise ratio remained constant. We performed some measurements also

in the absence of TiO₂ functionalization of the microwells (Fig. 4). In this case, the absolute fluorescence values increased, but the difference between positive signal and controls became lower (roughly 2:1, instead of 4:1 Fig. 4). Also, in this case, the absolute fluorescence signals measured when the mammalian cells were immunocaptured by bacteria displaying the specific anti-HER2 nanobody A10 were higher than those detected when the same cells were simply pelleted. As above, the background values were higher, whereas the ratio of the fluorescence intensity between target and control experiments remained constant. The use of A10-GFP soluble fluobodies (0.5 μg/well) instead of fluorescent bacteria displaying the same nanobody did not result in meaningful differences of fluorescence intensity when applied for SKBR3 cell detection (Fig. 4 yellow columns).

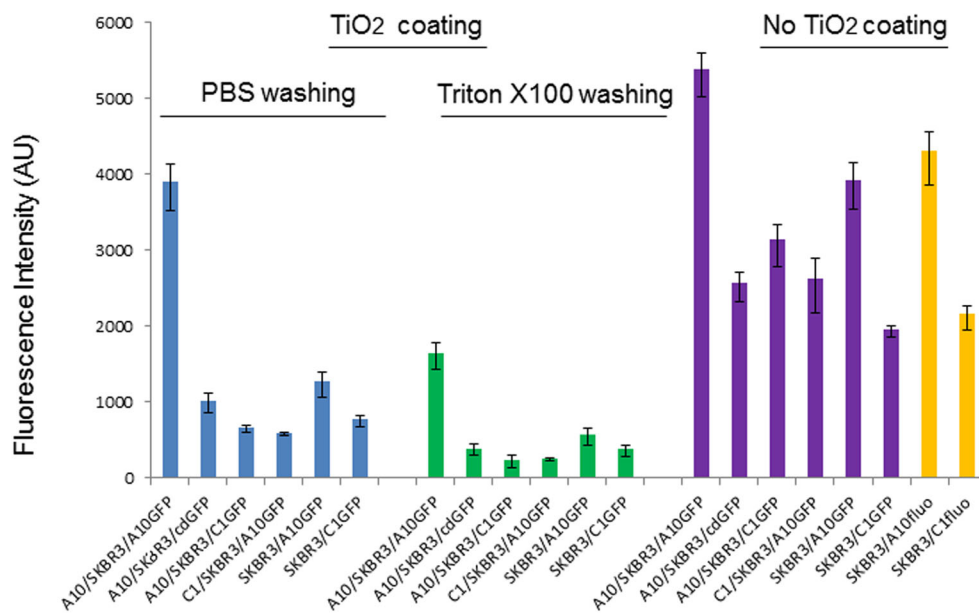


Fig. 4 Effect of washing conditions and TiO₂ coating on the specific detection of SKBR3 pos cells with bacteria displaying anti-HER2 bacteria. Non-fluorescent bacteria displaying the anti-HER2 nanobody A10 (capturing bacteria) were incubated with HER2 pos SKBR3 mammalian cells. As detection reagents, fluorescent bacteria displaying the same anti-HER2 nanobody (detection bacteria, A10GFP) were used. Controls were (i) detection fluorescent bacteria displaying the irrelevant enzyme FDH (cdGFP); (ii) detection bacteria displaying the irrelevant nanobody C1-GFP (anti-microalgae VHH); (iii) capturing bacteria displaying the

irrelevant nanobody C1 in combination with A10GFP detection bacteria; (iv) absence of capture bacteria in combination with A10GFP detection bacteria; (v) absence of capture bacteria and detection bacteria displaying the irrelevant nanobody C1. The same set of experiments was performed either changing the washing conditions (PBS or 0.1% Triton X-100 in PBS) or using wells not coated with TiO₂. In this last case, two more conditions were tested: (i) absence of capture bacteria and detection with soluble A10GFP fluobodies; (ii) absence of capture bacteria and detection with soluble irrelevant fluobody C1GFP

Finally, we evaluated a further combination of immunoreagents. HER2 pos mammalian cells (SKBR3) were immobilized by means of bacteria displaying the anti-HER2 nanobody A10 (Fig. S4) and visualized with soluble nanobodies fused to GFP (fluobodies). HER2 neg cells (MDA-MB231) were used as a negative control. In this case, when 50,000 cells/well were used the absolute fluorescence signal was above 30,000 but only twice the background (Fig. S4). We used this experimental set for assessing its limit-of-detection. The fluorescence signal-to-noise ratio strongly decreased when lower amounts of cells were used and the differences were no longer significant for samples with less than 12,500 cells, suggesting that the method could be more suitable for nanobody screening rather than for the capture and detection of rare mammalian cells. Control cells showed values of fluorescence intensity close to background at all the tested experimental conditions (Fig. S4).

The same capture-detection sandwich principle using pairs of nanobody-displaying bacteria (with and without GFP expression) was applied for the identification of toxic unicellular microalgae in combination with a nanobody (C1) which specifically recognizes *Alexandrium minutum*. The results shown in Fig. 3c indicate that the recognition was selective and required that both the anchoring and

detection bacteria displayed the C1 anti-*A. minutum* nanobody. In this case, the average fluorescence intensity reached almost the value of 12,000 whereas the negative controls did not exceed the threshold of 2000. Specifically, the negative control anti-HER2 nanobody A10 could neither stain *A. minutum* cells captured by C1 nor being used to capture the same cells for successive staining with C1-GFP (Fig. 3c). C1-displaying bacteria were successfully used also for identifying *A. minutum* cells by flow cytometry. This result confirmed the stability of the binding between nanobody-displaying bacteria and target cells, although the signal shift measured using this method was lower than that obtained with soluble fluobodies (Fig. 5). The controls (Fig. S5) confirmed that the signal was exclusively due to the specific binding between VHH and target cells since bacteria displaying irrelevant proteins showed no signal increase with respect to the background, irrespectively of their cytoplasmic GFP intensity. In contrast, we failed applying the bacterial display system to immunodetect extracellular vesicles (EVs) present in the medium of cultured cells by using the specific anti-EV H6 nanobody (Popovic et al. 2018). The absence of any clear signal increase above the background was probably due to the paucity of EVs in the samples, a result which implies insufficient sensitivity of the methodology.

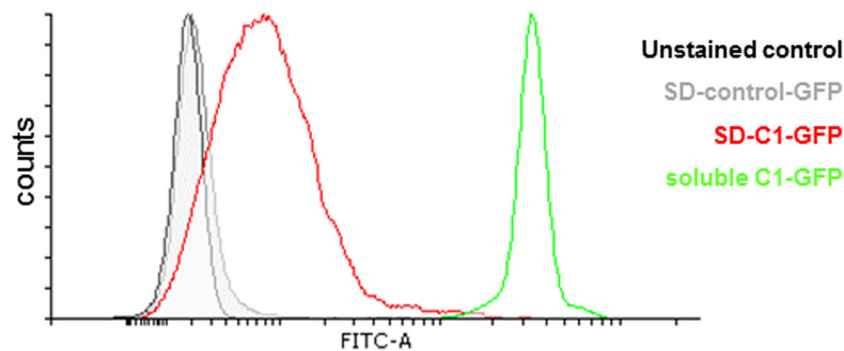


Fig. 5 Flow cytometry analysis of *Alexandrium minutum* cells stained with fluorescent bacteria displaying the specific C1 VHH. Algal cells were stained with fluorescent bacteria displaying C1 at their surface (SD-C1-GFP, red histogram). Negative controls are algae cells stained

with fluorescent bacteria displaying the irrelevant enzyme FDH (SD-control-GFP, gray histogram) and unstained cells (black histogram). The staining with soluble C1-GFP fluobodies (C1-GFP-soluble, green histogram) was included as a reference positive control

Discussion

Antibody production and correct display on solid surfaces are often laborious steps that require case-specific protocol optimization. We were able to show the proof-of-principle of an effective and simplified method to overcome them for the production of capture and diagnostic reagents. Nanobodies which recognize surface antigens can be conveniently expressed as functional binders displayed on bacteria surface. Such living immunoreagents are extremely convenient since they can be produced in just few hours by simple recombinant expression induction in liquid bacterial culture to be then directly used to functionalize solid surfaces for antigen capture in diagnostic applications. Once produced and used for coating a surface, activated bacteria remain functional for several weeks if conserved at 4 °C (De Marni et al. 2012). The antigen recognition can be performed by means of soluble fluobodies as well as by using fluorescent nanobody displaying bacteria, a condition that completely eliminates the need of purified reagents. As such, this last solution represents an alternative to other available tags used for protein functionalization (de Marco 2018) and a further development of methods which used binder displaying bacteria for immunocapture, but relied on fluorescent reagents for the antigen detection (Fleetwood et al. 2014; De Marni et al. 2012; Bong et al. 2018).

We set protocols for fluorescent-based detection of cancer cells and toxic microalgae in microplate format, microscopy, and flow cytometry. Further investigations are planned starting from purified and enriched EV fractions to elucidate the reasons of the deceiving results obtained when attempted detecting these biological components. Since their amount is normally low in the starting samples, we suspect that a large part of the bacterial surfaces remain available for non-specific interactions with contaminants resulting in high background. The nanobody display on bacteria is probably also not suitable for the identification of rare events, such as circulating cancer cells or diluted EV populations in biological samples, but it could be very convenient in applications in which it is

necessary to have robust, simple to produce, and inexpensive immunoreagents for repeated measurements of the targets, such as the monitoring of microalgae population fluctuations in environmental studies. Further studies are planned to determine dynamic range and limit-of-detection of nanobody-displaying bacteria in different diagnostic contexts and to identify the conditions that could improve these parameters. Another aspect for further investigations is the possibility to use nanobody-displaying bacteria for the immunocapture and concentration of biomarkers diluted in large volumes of biological samples (for instance, EVs from urine).

Finally, in this work, we showed that TiO₂ treatment is an effective alternative for increasing the adherence of bacteria on different plastic surfaces to the recently proposed solution of creating positive charges on the plastics to attract the negatively charged outer membrane of *E. coli* (Bong et al. 2018).

Acknowledgments The authors wish to thank Alfred Baran for having provided the microalgae strains.

Funding This work was supported by the grants ARRS/N4-0046 and ARRS/J4-9322 provided by the Javna agencija za raziskovalno dejavnost Republike Slovenije.

Compliance with ethical standards

Conflict of interests The authors declare that they have no conflict of interest.

Ethical approval This article does not contain any studies with human participants or animals performed by any of the authors.

References

- Aliprandi M, Sparacio E, Pivetta F, Ossolengo G, Maestro R, de Marco A (2010) The availability of a recombinant anti-SNAP antibody in VHH format amplifies the application flexibility of SNAP-tagged proteins. *J Biomed Biotechnol* ID 658954. doi: <https://doi.org/10.1155/2010/658954>

- Ambrosetti E, Paoletti P, Bosco A, Parisse P, Scaini D, Tagliabue E, de Marco A, Casalis L (2017) Quantification of circulating cancer biomarkers via sensitive topographic measurements on single binder nanoarrays. *ACS Omega* 2:2618–2629
- Berrow NS, Alderton D, Sainsbury S, Nettleship J, Assenberg R, Rahman N, Stuart DI, Owens RJ (2007) A versatile ligation-independent cloning method suitable for high-throughput expression screening applications. *Nucl Acids Res* 35:e45
- Bong JH, Song HW, Kim TH, Kang MJ, Jose J, Pyun JC (2018) Refolding of autodeployed anti-NEF scFv through oxidation with glutathione for immunosensors. *Biosens Bioelectron* 102:600–609
- Chauhan N, Kalal N, Juneja P, Punjabi PB (2016) Functionalized surfaces: bacterial adhesion. In: Mishra M (ed) *Encyclopedia of biomedical polymers and polymeric biomaterials*. Taylor and Francis, New York, pp 3509–3525
- Crepin R, Gentien D, Duché A, Rapinat A, Reyes C, Némati F, Massonnet G, Decaudin D, Djender S, Moutel S, Desrumeaux K, Cassoux N, Piperno-Neumann S, Amigorena S, Perez F, Roman Roman S, de Marco A (2017a) Nanobodies against surface biomarkers enable the analysis of tumor genetic heterogeneity in uveal melanoma patient derived xenografts. *Pigment Cell Melanoma Res* 30:317–327
- Crepin R, Veggiani G, Djender S, Beugnet A, Planeix F, Pichon C, Moutel S, Amigorena S, Perez F, Ghinea N, de Marco A (2017b) Whole-cell biopanning with a synthetic phage display library of nanobodies enabled the recovery of follicle-stimulating hormone receptor inhibitors. *Biochem Biophys Res Commun* 493:1567–1572
- de Marco A (2018) Nanomaterial bio-activation and macromolecules functionalization: the search for reliable protocols. *Protein Expr Purif* 147:49–54
- de Marco A, Deuerling E, Mogk A, Tomoyasu T, Bukau B (2007) Chaperone-based procedure to increase yields of soluble recombinant proteins produced in *E. coli*. *BMC Biotechnol* 7:32
- De Marni M, Monegal A, Venturini S, Vinati S, Carbone R, de Marco A (2012) Antibody purification-independent microarrays (PIM) by direct bacteria spotting on TiO₂-treated slides. *Methods* 56:317–325
- Djender S, Schneider A, Beugnet A, Crepin R, Desrumeaux K, Romani C, Moutel S, Perez F, de Marco A (2014) Bacterial cytoplasm as an effective cell compartment for producing functional VHH-based affinity reagents and *Camelidae* IgG-like recombinant antibodies. *Microb Cell Factories* 13:140
- Fleetwood F, Devoogdt N, Pellis M, Wernery U, Muyldermans S, Ståhl S, Löfblom J (2013) Surface display of a single-domain antibody library on gram-positive bacteria. *Cell Mol Life Sci* 70:1081–1093
- Fleetwood F, Andersson KG, Ståhl S, Löfblom J (2014) An engineered autotransporter-based surface expression vector enables efficient display of Affibody molecules on OmpT-negative *E. coli* as well as protease-mediated secretion in OmpT-positive strains. *Microb Cell Factories* 13:179
- Gratz A, Bollacke A, Stephan S, Nienberg C, Le Borgne M, Götz C, Jose J (2015) Functional display of heterotetrameric human protein kinase CK2 on *Escherichia coli*: a novel tool for drug discovery. *Microb Cell Factories* 14:74
- Gustavson M, Bäcklund E, Larsson G (2011) Optimisation of surface expression using the AIDA autotransporter. *Microb Cell Factories* 10:72
- Hoelsch K, Sührer I, Heusel M, Weuster-Botz D (2013) Engineering of formate dehydrogenase: synergistic effect of mutations affecting co-factor specificity and chemical stability. *Appl Microbiol Biotechnol* 97:2473–2481
- Jong WSP, Soprova Z, de Punder K, ten Hagen-Jongman CM, Wagner S, Wickström D, de Gier JW, Andersen P, van der Wel NN, Luirink J (2012) A structurally informed autotransporter platform for efficient heterologous protein secretion and display. *Microb Cell Factories* 11:85
- Jose J, Handel S (2003) Monitoring the cellular surface display of recombinant proteins by cysteine labeling and flow cytometry. *Chembiochem* 4:396–405
- Kranen E, Detzel C, Weber T, Jose J (2014) Autodisplay for the co-expression of lipase and foldase on the surface of *E. coli*: washing with designer bugs. *Microb Cell Factories* 13:19
- Krüger C, Hu Y, Pan Q, Marcotte H, Hultberg A, Delwar D, van Dalen PJ, Pouwels PH, Leer RJ, Kelly CG, van Dollenweerd C, Ma JK, Hammarström L (2002) *In situ* delivery of passive immunity by lactobacilli producing single-chain antibodies. *Nat Biotechnol* 20:702–706
- Lorenzetti M, Dogša I, Stošički T, Stopar D, Kalin M, Kobe S, Novak S (2015) The influence of surface modification on bacterial adhesion to titanium-based substrates. *ACS Appl Mater Interfaces* 7:1644–1651
- Marcotte H, Köll-Klais P, Hultberg A, Zhao Y, Gmür R, Mändar R, Mikelsaar M, Hammarström L (2006) Expression of single-chain antibody against RgpA protease of *Porphyromonas gingivalis* in *Lactobacillus*. *J Appl Microbiol* 100:256–263
- Massa PE, Panizza A, Monegal A, de Marco A, Rescigno M (2013) Salmonella engineered to express CD20-targeting antibodies and a drug-converting enzyme can eradicate human lymphomas. *Blood* 122:705–714
- Mazzega E, Beran A, Cabrini M, de Marco A (2018) *In vitro* isolation of nanobodies for selective *Alexandrium minutum* recognition: a model for convenient development of dedicated immuno-reagents to study and diagnostic toxic unicellular algae. *Harmful Algae* 82:44–51
- Michon C, Langella P, Eijsink VG, Mathiesen G, Chatel JM (2016) Display of recombinant proteins at the surface of lactic acid bacteria: strategies and applications. *Microb Cell Factories* 15:70
- Monegal A, Ami D, Martinelli C, Huang H, Aliprandi M, Capasso P, Francavilla C, Ossolengo G, de Marco A (2009) Immunological applications of single domain llama recombinant antibodies isolated from a naïve library. *Protein Eng Des Sel* 22:273–280
- Moutel S, Bery N, Bernard V, Keller L, Lemesre E, de Marco A, Ligat L, Rain JC, Favre G, Olichon A, Perez F (2016) NaLi-H1: a universal synthetic library of humanized nanobodies providing highly functional antibodies and intrabodies. *eLife*. <https://doi.org/10.7554/eLife.16228>
- Nhan NT, de Valdivia EG, Gustavsson M, Hai TN, Larsson G (2011) Surface display of *Salmonella* epitopes in *Escherichia coli* and *Staphylococcus carnosus*. *Microb Cell Factories* 10:22
- Park M, Yoo G, Bong J-H, Jose J, Kang MJ, Pyun JC (2015) Isolation and characterization of the outer membrane of *Escherichia coli* with autodeployed Z-domains. *Biochim Biophys Acta Biomembr* 1848:842–847
- Popovic M, Mazzega E, Toffoletto B, de Marco A (2018) Isolation of anti-extra-cellular vesicle single-domain antibodies by direct panning on vesicle-enriched fractions. *Microb Cell Factories* 17:6
- Quehl P, Hollender J, Schüürmann J, Brossette T, Maas R, Jose J (2016) Co-expression of active human cytochrome P450 1A2 and cytochrome P450 reductase on the cell surface of *Escherichia coli*. *Microb Cell Factories* 15:26
- Quehl P, Schüürmann J, Hollender J, Jose J (2017) Improving the activity of surface displayed cytochrome P450 enzymes by optimizing the outer membrane linker. *Biochim Biophys Acta Biomembr* 1859:104–116
- Salema V, Mañas C, Cerdán L, Piñero-Lambea C, Marín E, Roovers RC, Van Bergen En Henegouwen PM, Fernández LÁ (2016) High affinity nanobodies against human epidermal growth factor receptor selected on cells by *E. coli* display. *MAbs* 8:1286–1301
- Schüürmann J, Quehl P, Festel G, Jose J (2014) Bacterial whole-cell biocatalysts by surface display of enzymes: toward industrial application. *Appl Microbiol Biotechnol* 98:8031–8046

- Shao X, Jiang M, Yu Z, Cai H, Li L (2009) Surface display of heterologous proteins in *Bacillus thuringiensis* using a peptidoglycan hydrolase anchor. *Microb Cell Factories* 8:48
- Sichwart S, Tozakidis IE, Teese M, Jose J (2015) Maximized autotransporter-mediated expression (MATE) for surface display and secretion of recombinant proteins in *Escherichia coli*. *Food Technol Biotechnol* 53:251
- Sührer I, Langemann T, Lubitz W, Weuster-Botz D, Castiglione K (2015) A novel one-step expression and immobilization method for the production of biocatalytic preparations. *Microb Cell Factories* 14:180
- Tozakidis IEP, Sichwart S, Jose J (2015) Going beyond *E. coli*: autotransporter based surface display on alternative host organisms. *New Biotechnol* 32:644–650
- Veggiani G, de Marco A (2011) Improved quantitative and qualitative production of single-domain intrabodies mediated by the co-expression of Erv1p sulfhydryl oxidase. *Protein Expr Purif* 79:111–114
- Veggiani G, Ossolengo G, Aliprandi M, Cavallaro U, de Marco A (2011) Single-domain antibodies that compete with the natural ligand fibroblast growth factor block the internalization of the fibroblast growth factor receptor 1. *Biochem Biophys Res Commun* 408:692–696
- Wieczorek AS, Martin VJJ (2010) Engineering the cell surface display of cohesins for assembly of cellulosome-inspired enzyme complexes on *Lactococcus lactis*. *Microb Cell Factories* 9:69
- Yoo G, Park M, Lee E-H, Jose J, Pyun J-C (2011) Immobilization of *E. coli* with autodisplayed Z-domains to a surface-modified microplate for immunoassay. *Anal Chim Acta* 707:142–147
- Zou T, Dembele F, Beugnet A, Sengmanivong L, Trepout S, Marco S, de Marco A, Li M-H (2015) Nanobody-functionalized PEG-b-PCL polymersomes and their targeting study. *J Biotechnol* 214:147–155

Publisher's note Springer Nature remains neutral with regard to jurisdictional claims in published maps and institutional affiliations.